The Effect of the Flexibility of a Bridge on the Passenger Comfort of a Travelling Vehicle Including Road Roughness

[1]İsmail Esen and *[2]Mehmet Akif Koc
[1]Faculty of Engineering, Department of Mechanical Engineering Karabuk University, Turkey
*[2]Faculty of Technology, Department of Mechanical Engineering Sakarya University, Turkey

Abstract

In this study, the effect of the flexibility of a bridge on the passenger comfort for a travelling half model car with six degrees of freedom has been investigated. The coupled equation of motion of vehicle and the bridge was obtained using the Lagrange's equation, and then was solved using the fourth degree Runge-Kutta method with a special software written in MATLAB®. The vehicle model considered in this study includes tires, suspension system, and car body and driver and passenger seats. The road roughness functions for different asphalt qualities were obtained using ISO-8608 road quality standard. The bridge has been modelled as an Euler-Bernoulli beam. Thus, considering different road classes the effect of the bridge flexibility on the passenger comfort was studied.

Key words: Bridge flexibility, road roughness, passenger comfort, vehicle bridge interaction, ISO-8608.

1. Introduction

Dynamic interaction of the structures with moving loads is an important subject in several engineering fields such as civil, mechanical, aviation etc. The subject have many different aspects according to the engineering applications so that one can find a wide variety of the use of it through the studies [1-17]. In transportation engineering dynamic interaction of vehicles and bridges have also been studied in the field of well-known VBI (Vehicle Bridge Interaction) problems like [18]. Especially heavy load trucks and high-speed trains emerges the new studies. The effects of several parameters of the vehicles like suspension systems, vehicle velocity, acceleration and deceleration of vehicle, the properties of the bridge on the interaction have been presented by [19-26]. The studies on the effect of the flexibility of the bridges on the passenger comfort are limited. In this study, the effect of the bridge flexibility along with road roughness on the car dynamics is widely studied. The dynamics of the car body, the suspension system and driver and passenger seats have been analysed and presented.

2. Theory

2.1. Determination vehicle-bridge coupled equations

For the effects of VBI on vehicle dynamics, a six-DOF half car model on a flexible bridge with road roughness, given in Figure 1 is studied. In general the dynamics of the vehicle and the

*Corresponding author: Address: Faculty of Technology, Department of Mechanical Engineering Sakarya University, 54187, Sakarya TURKEY. E-mail address: makoc@sakarya.edu.tr, Phone: +902642955752 Fax: +902642955601

bridge can be analysed trough uncoupled equations of motions of each parts of vehicle and bridge systems. In this study the motion equation of both the car and the bridge will be coupled trough the state space equation. Considering more realistic analysis results the model of the vehicle was well set up. The half car model consists of car body, elastically mounted driver and passenger seats, front and rear suspension systems with elastic tires. In Figure 1, k_{t1}, k_{t2}, k_1, k_2, k_{y1}, k_{y2}, respectively, are the stiffness coefficients of front tire, rear tire, front suspension, rear suspension, driver sea and passenger seat. The symbols c_{t1}, c_{t2}, c_1, c_2, c_{y1}, c_{y2} represents the damping coefficients in the same order. The masses, m_{t1}, m_{t2}, m_a, m_{y1}, m_{y2}, respectively are the mass of the front suspension, rear suspension including tires, car body, driver and passenger masses. Parameters y_{t1}, y_{t2}, y_a, y_{y1}, y_{y2} are the dynamic displacements of front tire, rear tire, car body, driver seat and passenger seats respectively, while θ represents the rotation of car body about the mass centre and generally is called as pitch motion. Vertical deflections of the bridge is represented by y*(x, t)*, and the road roughness is represented by r*(x)*.

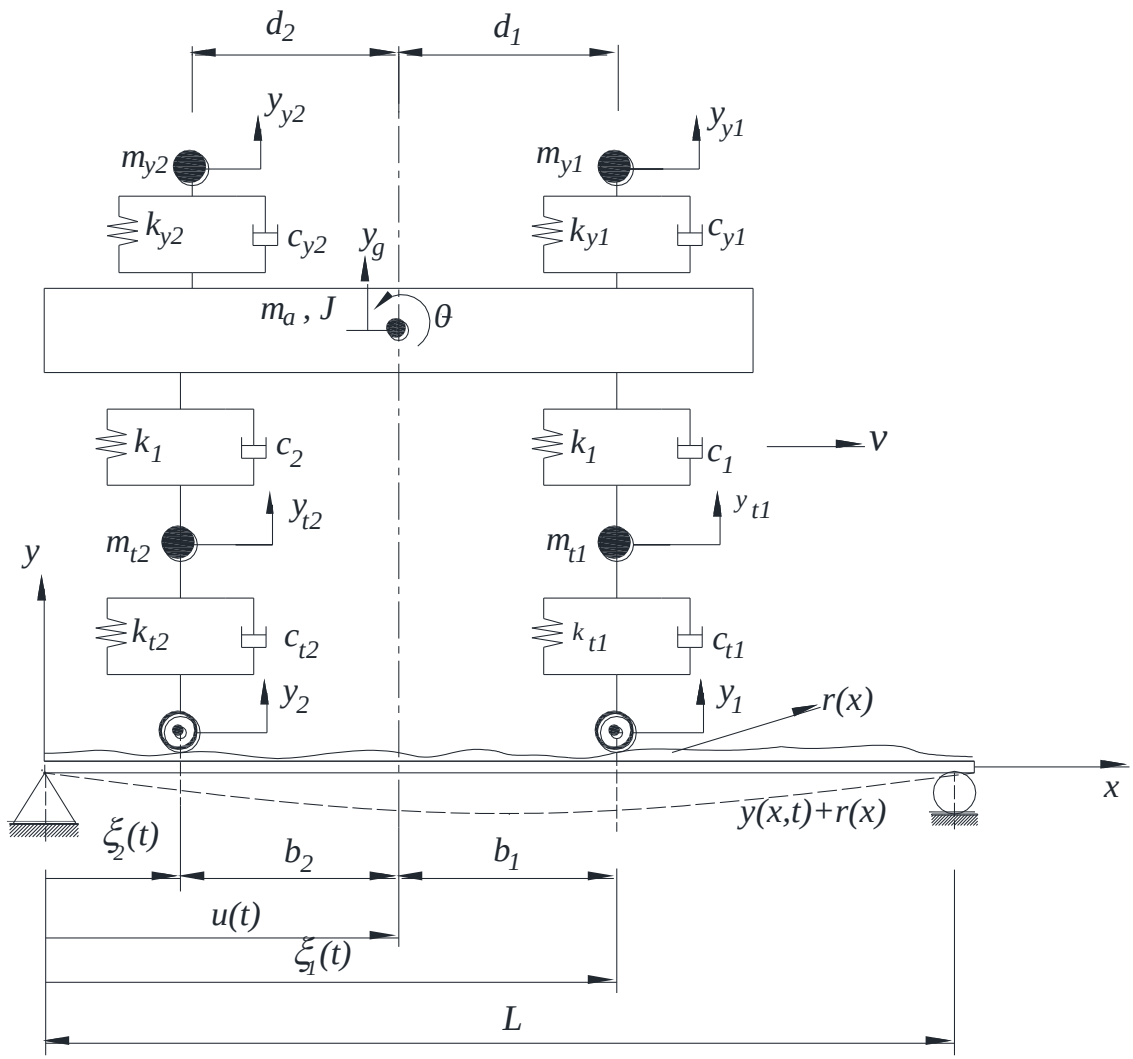

Figure 1. Vehicle-bridge interaction model with road roughness

Considering above assumptions the total kinetic and potential energies of bridge and the vehicle can be given by:

$$E_k = \frac{1}{2}\left\{\int_0^L \rho\left[\dot{y}^2(x,t)\right]dx + m_a\dot{y}_a^2(t) + J\dot{\theta}^2(t) + m_{y1}\dot{y}_{y1}^2(t) + m_{y2}\dot{y}_{y2}^2(t) + m_{t1}\dot{y}_{t1}^2(t) + m_{t2}\dot{y}_{t2}^2(t)\right\},$$

$$E_p = \frac{1}{2}\left\{\int_0^L EI[y''^2(x,t)dx] + k_{y1}[y_a(t) + d_1\theta(t) - y_{y1}(t)]^2 + k_{y2}[y_a(t) + d_2\theta(t) - y_{y2}(t)]^2 + k_1[y_a(t) + b_1\theta(t) - y_{t1}(t)]^2\right. \quad (1)$$

$$\left. + k_2[y_a(t) - b_2\theta(t) - y_{t2}(t)]^2 + k_{t1}[y_{t1}(t) - y(\xi_1(t),t)]^2 H(x,\xi_1(t)) + k_{t2}[y_{t2}(t) - y(\xi_2(t),t)]^2 H(x,\xi_2(t))\right\},$$

Where ρ is the unit mass of the bridge beam, *EI* is the rigidity of the beam and *H(x)* represents the Heaviside function. The coordinates of the tires on the bridge are $\xi_1(t) = u(t) + b_1, \quad \xi_2(t) = u(t) - b_2,$ Using Lagrange principle and Galerkin's approximation for deflection of the bridge beam and orthogonality of the modes taken into account the equations below can be obtained as:

$$y(x,t) = \sum_{i=1}^{n}\phi_i(x)q_i(t), \quad \phi_i(x) = \sqrt{\frac{2}{L}}\sin\left(\frac{i\pi x}{L}\right), \quad i = 1,2,...,n., \int_0^L \rho\phi_i(x)\phi_j(x)dx = \Omega_i\delta_{ij}, \int_0^L EI\phi_i''(x)\phi_j''(x)dx = \Pi_i\delta_{ij},$$

(2)

Where q_i (t) are modal coordinates. The gravitational contact forces of the each tire are:

$$f_s(x,t) = -(f_{s1}H(x-\xi_1(t))) + (f_{s2}H(x-\xi_2(t))), \; f_{s1} = \left(m_{t1} + m_a\frac{b_2}{b_1+b_2} + m_{y1}\frac{b_2+d_1}{b_1+b_2} + m_{y2}\frac{b_2-d_2}{b_1+b_2}\right)g,$$

$$f_{s2} = \left(m_{t2} + m_a\frac{b_1}{b_1+b_2} + m_{y1}\frac{b_1-d_1}{b_1+b_2} + m_{y2}\frac{b_1+d_2}{b_1+b_2}\right)g, \quad (3)$$

Rayleigh dissipation function for whole system is [17]:

$$R = \frac{1}{2}\left\{c\dot{y}^2(x,t) + c_{y1}[\dot{y}_a(t) + d_1\dot{\theta}(t) - \dot{y}_{y1}(t)]^2 + c_{y2}[\dot{y}_a(t) - d_2\dot{\theta}(t) - \dot{y}_{y2}(t)]^2 + c_1[\dot{y}_a(t) + b_1\dot{\theta}(t) - \dot{y}_{t1}(t)]^2\right. \quad (4)$$

$$\left. + c_2[\dot{y}_a(t) - b_2\dot{\theta}(t) - \dot{y}_{t2}(t)]^2 + c_{t1}[\dot{y}_{t1}(t) - \dot{y}(\xi_1(t),t)]^2 H(x-\xi_1(t)) + c_{t2}[\dot{y}_{t2}(t) - \dot{y}(\xi_2(t),t)]^2 H(x-\xi_2(t))\right\},$$

Using Lagrange equations below for whole system considering six state variables $p(t) = \left\{y_a(t) \;\; \theta(t) \;\; y_{y1} \;\; y_{y2} \;\; y_{t1} \;\; y_{t2}\right\}^T$, and *Qi* generalized force $Q_i = \int_0^L \phi_i(x) f_g(x,t)dx, \;\; i = 1,2,...,n.$,

$$\frac{\mathrm{d}}{\mathrm{d}t}\left(\frac{\partial E_k}{\partial \dot{p}_k(t)}\right) - \frac{\partial E_k}{\partial p_k(t)} + \frac{\partial E_p}{\partial p_i(t)} + \frac{\partial R}{\partial \dot{p}_k(t)} = 0 \text{ , } k = 1,2,....,6, \quad \frac{\mathrm{d}}{\mathrm{d}t}\left(\frac{\partial E_k}{\partial \dot{q}_i(t)}\right) - \frac{\partial E_k}{\partial q_i(t)} + \frac{\partial E_p}{\partial q_i(t)} + \frac{\partial R}{\partial \dot{q}_i(t)} = Qi \text{ , i} = 1,2,....,n,$$

(5)

One can obtain the equation of motion for driver and passenger seats as given below:

$$\begin{aligned} &m_{y1}\ddot{y}_{y1} + c_{y1}[\dot{y}_{y1}(t) - \dot{y}_a(t) - d_1\dot{\theta}(t)] + k_{y1}[y_{y1}(t) - y_a(t) - d_1\theta(t)] = 0, \\ &m_{y2}\ddot{y}_{y2} + c_{y2}[\dot{y}_{y2}(t) - \dot{y}_a(t) + d_2\dot{\theta}(t)] + k_{y2}[y_{y2}(t) - y_a(t) + d_2\theta(t)] = 0, \end{aligned} \tag{6}$$

For other parts of the vehicle the motion equations one can refer to [17 and 28]. The bridge response is described by *n* independent second order differential equations given by

$$\begin{aligned} &\Omega_i\ddot{q}_i(\mathrm{t}) + \Pi_i q_i(\mathrm{t}) + \Lambda_1\phi_i(\xi_1(\mathrm{t}))\left\{ f_{s1} + c_{t1}\left[\dot{y}(\xi_1(\mathrm{t}),\mathrm{t})\Lambda_1 - \dot{y}_{t1}(\mathrm{t})\right] + k_{t1}\left[y(\xi_1(\mathrm{t}),\mathrm{t})\Lambda_1 - \mathrm{y}_{t1}(\mathrm{t})\right]\right\} \\ &+\Lambda_2\phi_i(\xi_2(\mathrm{t}))\left\{ f_{s2} + c_{t2}\left[\dot{y}(\xi_2(\mathrm{t}),\mathrm{t})\Lambda_2 - \dot{y}_{t2}(\mathrm{t})\right] + k_{t2}\left[y(\xi_2(\mathrm{t}),\mathrm{t})\Lambda_2 - y_{t2}(\mathrm{t})\right]\right\} = 0 \quad i = 1,2,\ldots,n, \\ &0 \le t < t_1\text{: } \Lambda_1 = 1, \Lambda_2 = 0;\ t_1 \le t < t_2\text{: } \Lambda_1 = 1, \Lambda_2 = 1;\ \ t_2 \le t < t_3\text{: } \Lambda_1 = 0, \Lambda_2 = 1;\ \ t_3 \le t\text{: } \Lambda_1 = 0, \Lambda_2 = 0, \end{aligned} \tag{7}$$

The above equations can be represented in the state space form as

$$\dot{x}(t) = A(t)x(t) + f(t), \tag{8}$$

The expressions in above equation that are given in the Appendix A. are also can be found from [17 and 28].

2.2. Road roughness model

If there is no contact loss between the upper vehicle and the bridge surface, the deflection, velocity and accelerations of each tire is obtained by adding the roughness function r(x) to the bridge deflection y(x, t), and then for velocity first order, for acceleration second order differentiating with respect to time, as seen below

$$y_1(t) = y_1(x,t) + r_1(x),\ \ y_2(t) = y_2(x,t) + r_2(x), \tag{9}$$

$$\begin{aligned} &\dot{y}_1(t) = \frac{\mathrm{d}y(t)}{\mathrm{d}t} = \left\{ \frac{\partial y}{\partial t} + \left(\frac{\mathrm{d}x}{\mathrm{d}t}\right)\frac{\partial y}{\partial x} + r\frac{\partial r}{\partial x} \right\}_{y=y_1, x=\xi_1, r=r_1}, \\ &\ddot{y}_1(t) = \frac{\mathrm{d}^2 y(t)}{\mathrm{d}t} = \left\{ \frac{\partial^2 y}{\partial t^2} + 2\left(\frac{\mathrm{d}x}{\mathrm{d}t}\right)\frac{\partial^2 y}{\partial x \partial t} + \left(\frac{\mathrm{d}x}{\mathrm{d}t}\right)^2 \frac{\partial^2 y}{\partial x^2} + \left(\frac{\mathrm{d}^2 x)}{\mathrm{d}t^2}\right)\frac{\partial y}{\partial x} + \left(\frac{\mathrm{d}x}{\mathrm{d}t}\right)^2 \frac{\partial^2 r}{\partial x^2} + \left(\frac{\mathrm{d}^2 x}{\mathrm{d}t^2}\right)\frac{\partial r}{\partial x} \right\}_{y=y_1, x=\xi 1, r=r_1}, \\ &\text{where, } \left(\frac{\mathrm{d}x}{\mathrm{d}t}\right) = v,\ \ \left(\frac{\mathrm{d}^2 x}{\mathrm{d}t^2}\right) = a \end{aligned} \tag{10}$$

For the second tire the velocity and acceleration are obtained by the same manner as the first one using appropriate coordinates, where $y=y_2$, $x=\xi_2$ and $r=r_2$.

For the evaluation of r(x), the one can use ISO-8608 standard [25]. The Power Spectral Density (PSD) function have been used for obtaining the surface profile in terms of road classes which is given in Table 1.

Table 1. ISO-8608 for values $G_d(n_0)$ [27]

	$G_d(n_0)$ (10^{-6} m^3)	
	lower limit	upper limit
A	-	32
B	32	128
C	128	512
D	512	2048
E	2048	8192
F	8192	32768
G	32768	131072
H	131072	-
n_o=0:1 cycles/m		

Accordingly the PSD function for road roughness is given by

$$G_d(n) = G_d(n_0)\left(\frac{n}{n_0}\right)^{c} \quad (n_0 = 0\text{-}1) \tag{11}$$

where n_0 reference spatial frequency 0,1 (cycle/metre) and c is the power of PSD and for a constant velocity of the vehicle $c=2$. The symbol n is spatial frequency (cycle/s) and $G_d(n_0)$ will be evaluated according to the road class using Table 1. Using inverse Fourier for Eq. (13) the spatial roughness function r(x) is given by

$$r(\mathrm{x}) = \sum_{i=1}^{N} \sqrt{4G_d(\mathrm{n}_i)\Delta n}\cos(2p\,\mathrm{n}_i\mathrm{x} + q_i) \tag{12}$$

Where q_i is the random phase angle between 0 and 2π, and Δn is the frequency increment with $\Delta n = (n_{\max} - n_{\min})/N$, where N, is the total frequency step between n_{min} and n_{max}. While n_i frequency value is calculated using $n_i = n_{min} + \Delta n(i-1)$. The calculation algorithm of such r(x) is given in Table 2 using notations of MATLAB (in Appendix A), where v, t_0, t_{end} and Δt respectively are the constant velocity of the vehicle, the beginning time, the end time and the time increment.

3. Numerical analysis and discussions

For analysis of the interaction and passenger comfort the bridge and vehicle were modelled using the parameters given below.

Bridge:
L=100 m, E=207 Gpa, I=0.174 m^4,ρ=20 000 kg/m, c=1750 Ns/m,
Vecihle:
m_a=1794.4 kg, m_{t1}=87.15, m_{t2}=140.4, m_{p1}= m_{p2}=75 kg, J=3443.05 kg m^2, b_1=1.271, b_2=1.716, d_1=0.481, d_2=1.313 m, k_1=66824.4, k_2=18615.0, k_{t1}= k_{t2}=101115.0, k_{p1}=k_{p2}=14000.0 N/m, c_1=1190, c_2=1000, c_{t1}= c_{t2}=14.6, c_{p1}=50.2, c_{p2}=62.1 Ns / m , v=72 km/h.

In calculation of the deflections of the bridge the first four vibration mode were taken into account considering the effects of the higher modes would rapidly be damped out by damping. The effect of the flexibility of the bridge was modelled using the rigidity *EI*. The accelerations of the passenger seat, vehicle body and the front tire are shown in Figure 2 for road classes A and B.

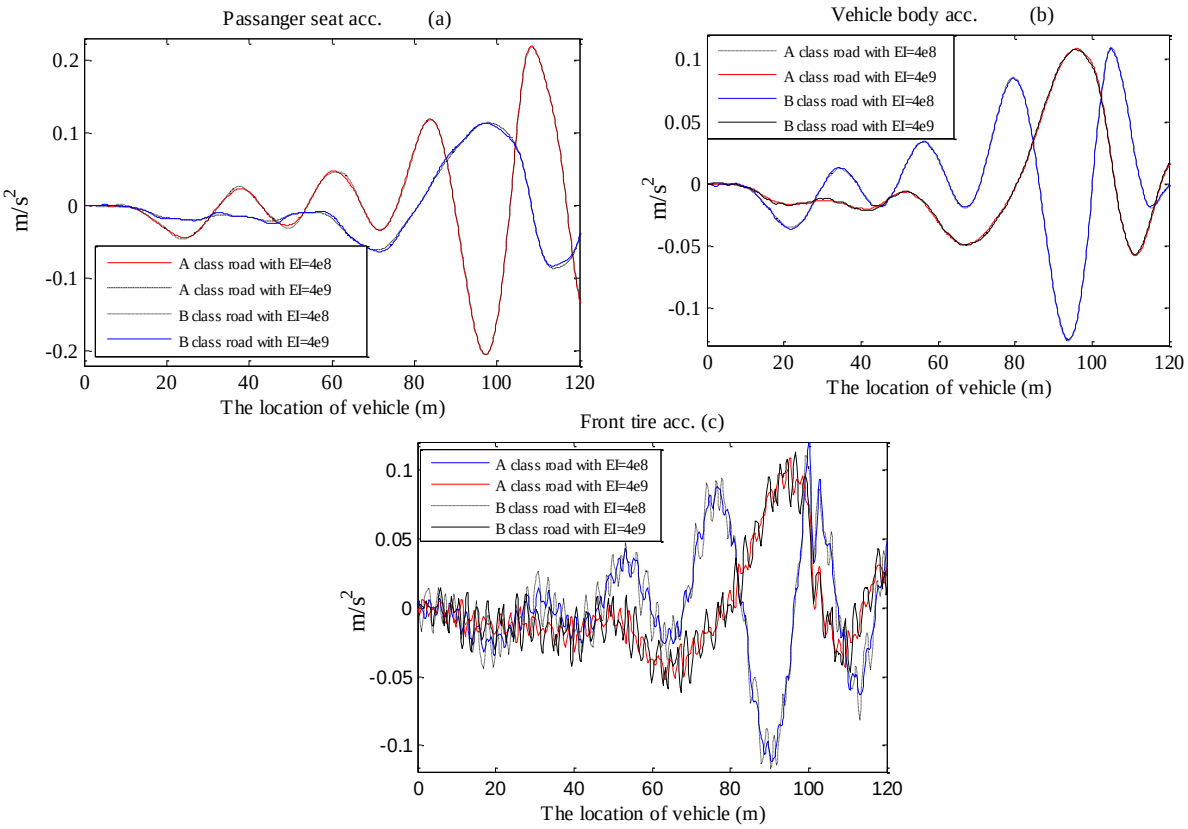

Figure 2. Vehicle accelerations (m/s^2) for different road roughness (A, B) and bridge flexibility, a) passenger seat, b) vehicle body, c) front tire

From the close examination of Figure 2 one can realise that on the accelerations of the vehicle, the rigidity of the bridge is more effective than the road roughness. The effect of the roughness can be accepted meaning full when the dynamics of the tire is important for the road classes A and B. Figure 3 shows the accelerations for the road classes C and D and for different rigidity. The same behaviour can be seen as the A and B classes that the rigidity is dominant in the dynamic interaction of the vehicle and bridge. As an interesting behaviour of the vehicle-bridge interaction, the accelerations are generally increasing while the vehicle travelling on the bridge. The maxima of the accelerations were occurred after the vehicle passed the midpoint of the bridge. This is caused by the change of the dynamic deflection shape of the bridge depending on the different rigidity. The reasons of this kind of behaviour of the bridge have been widely studied in previous studies like [1, 2 and 12]. Figure 4 depicts the dynamic interaction for the bridge flexibilities. Generally, the more the rigidity increases the less the accelerations occurs.

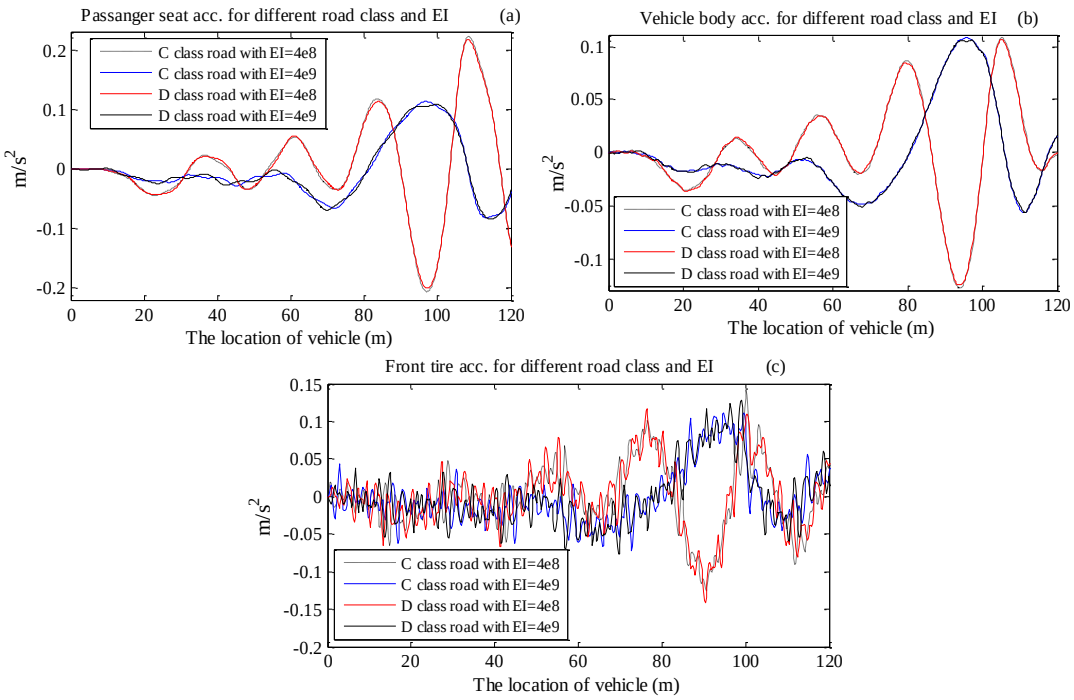

Figure 3. Vehicle accelerations (m/s^2) for different road roughness (C, D) and bridge flexibility, a) passenger seat, b) vehicle body, c) front tire

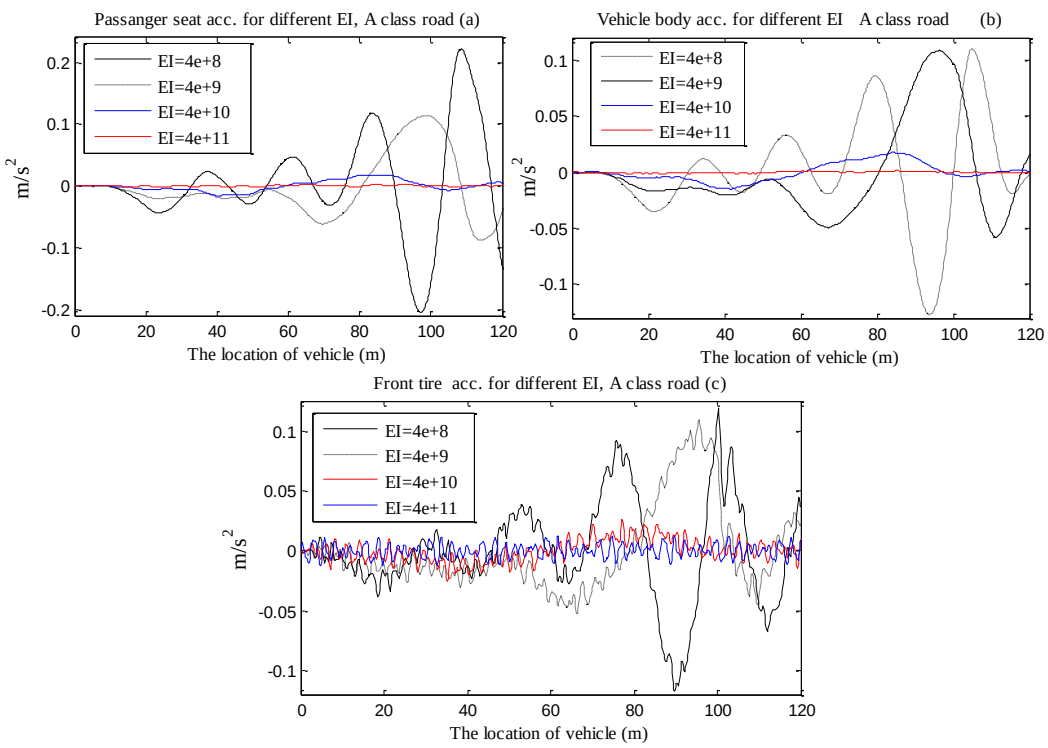

Figure 4. Vehicle accelerations (m/s^2) for A class road roughness (A, B) and different bridge flexibility ($4x10^8$,$4x10^9$, $4x10^{10}$, $4x10^{11}$), a) passenger seat , b) body, c) front tire.

Conclusions

- Considering vehicle dynamics, the rigidity of the bridge is more effective than the road roughness.
- The effect of the roughness should be taken into account when the dynamics of the tire is important.

References

[1] Fryba L. Vibration solids and structures under moving loads. London: Thomas Telford House 1999.

[2] Bajer I. C., Dyniewicz B. Numerical Analysis of Vibrations of Structures Under Moving Inertial Load, Springer, 2012.

[3] S. Timeshenko,D. Young and W. Weaver, Vibration problems in Engineering, 4th edition (John Wiley, New York, 1974)

[4] Esen, İ., Gerdemeli, İ., 2010,"Hareketli Yükler Altındaki Köprülü Kren Kirişlerinin Dinamik Analizi",İtü dergisi/d, Vol.9 pp.145-156.

[5] Dyniewicz, B., & Bajer, C. (2012). New consistent numerical modelling of a travelling accelerating concentrated mass. World J Mech, 2 (6), 281-287.

[6] Lee, H., P. (1996). Transverse vibration of a Timoshenko beam acted upon by an accelerating mass. Appl Acoust, 47 (4), 319-330.

[7] Michaltsos, G. (2002). Dynamic behaviour of a single-span beam subjected to loads moving with variable speeds. J. Sound Vib., 258 (2), 359-372.

[8] Wang, Y. M. (2009). The transient dynamics of a moving accelerating/decelerating mass travelling on a periodic-array non-homogeneous composite beam. Eur. J. Mech. A. Solids., 28, 827-840.

[9] Dehestani, M., Mofid M., & Vafai, A. (2009). Investigation of critical influential speed for moving mass problems on beams. Appl. Math. Modell., 33(10), 3885-3895.

[10] Michaltsos, G., Sophianopoulos, D., & Kounadis, A. N. (1996). The effect of a moving mass and other parameters on the dynamic response of a simply supported beam. J. Sound Vib., 191(3), 357-362

[11] Esen, İ. (2013). A new finite element for transverse vibration of rectangular thin plates under a moving mass. Finite Elem. Anal. Des., 66, 26-35.

[12] Esen, İ. (2011). Dynamic response of a beam due to an accelerating moving mass using moving finite element approximation. Math Comput Appl, 16(1), 171-182.

[13] Kahya, V. (2012). Dynamic analysis of laminated composite beams under moving loads using finite element method. Nucl. Eng. Des., 243, 41-48.

[14] Esen, İ., Koç, M., A., 2013, "Dynamics of 35 mm Anti-aircraft Cannon Barrel During Firing", İnternational Symposium on Computing in Science, İSCSE 201324-25 Ekim, Aydın.

[15] Esen, İ., Koç, M., A., "35 mm Uçaksavar Topu Namlusu için Titreşim Absorberi Tasarımı ve Genetik Algoritma ile Optimizasyonu", Otomatik Kontrol Ulusal Toplantısı, TOK2013, 26-28 Eylül 2013, Malatya, Türkiye, pp. 513-518.

[16] Esen, İ., Koc, M. A., "Optimization a passive vibration absorber for a barrel using genetic algorithm",Expert Systems with Applications, 42(2015) 894-905

[17] Esmailzadeh, E., Jalili, N.,2002, "Vehicle-Passenger-Structure Interaction of Uniform Bridges Traversed by Moving Vehicles ", Journal of Sound and Vibration, Vol. 260, pp. 611-635.

[18] M. Fafard, M. Bennur, M. Savard, A general multi-axle vehicle model to study the bridge-vehicle interaction. Engineering Computation 14(5) (1997) 491-508.

[19] Lou, P., 2005,"A Vehicle-Track-Bridge Interaction Element Considering Vehicle's Pitching Effect",Finite Element in Analysis and Design, Vol. 41 pp. 397-427.

[20] Yang, Y., B., Cheng, M., C., Chang, K., C.,2012, "Frequency Variation in Vehicle-Bridge Interaction Systems", International Journal of Structural Stability and Dynamics, Vol. 13 pp. 397-427.

[21] Azimi, H., Galal, K., Pekau, O., A., 2013 "A Numerical Element for Vehicle-Bridge Interaction Analysis of Vehicles Experiencing Sudden Deceleration", Engineering Structures, Vol. 49 pp. 792-805.

[22] Lou, P.,Au, F., 2013, "Finite Element Formula efor Internal forces of Bernoulli-Euler Beams Under Moving Vehicles", Journal of Sound and Vibration, Vol. 332 pp. 1533-1552.

[23] Belyaev A. K., Irschik H. and Krommer M. Mechanics and Model-Based Control of Advanced Engineering Systems, Springer, 2014.

[24] Uys, P. E., Els, P. S., Thoresson, M., Suspension setting for optimal ride comfort of off-road vehicles travelling on roads with different roughness and speeds, 44(2007) 163-175.

[25] Law, S., S., Zhu, X. Q., Bridge dynamic response due to road surface roughness and braking of vehicle

[26] Optimal Design of Passenger Car Suspension for ride and road holding

[27] Agostinacchio A., Ciampa D., Olita S., "The Vibrations induced by surface irregularities in road pavements – a Matlab approach", Eur. Transp. Res. Rev, (2014)6:267-275.

[28] Esen İ. ve Koc M. A. Araç köprü etkileşiminin yolcu konforu üzerine etkisinin modellenmesi, 4. Otomotiv Teknolojileri Kongresi, Bursa, 01-04 Haziran 2008

Appendix A.

The parameters of the Eq. (8) are given below [17 and 28]:

$$x(\mathrm{t}) = \begin{Bmatrix} x_1(\mathrm{t}) \\ \dot{x}_1(\mathrm{t}) \end{Bmatrix}, x_1(t) = \{ p^T(t) \;\; q_1(t) ... q_n(t) \}^T, \tag{A.1}$$

$$A=\begin{bmatrix} & 0_{(n+6)x(n+6)} & & I_{(n+6)x(n+6)} & & \\ K_{6x6} & & 0_{6x6} & C_{6x6} & & 0_{6xn} \\ 0_{nx4} & V_{nx2} & \Pi_{nxn} & 0_{nx4} & \Theta_{nx2} & \Upsilon_{nxn} \end{bmatrix}_{2(n+6)x2(n+6)}, \tag{A.2}$$

$$f(t)=\begin{bmatrix} 0_{(n+12)x1} \\ P_{nx1} \end{bmatrix}_{2(n+6)x1}, \tag{A.3}$$

Where K_{6x6} is the stiffness and C_{6x6} is the damping matrices of the vehicle.

$$V=\begin{bmatrix} k_{t1}\Lambda_1\phi_1(\xi_1(t)) & k_{t2}\Lambda_2\phi_1(\xi_2(t)) \\ \vdots & \vdots \\ k_{t1}\Lambda_1\phi_n(\xi_1(t)) & k_{t2}\Lambda_2\phi_n(\xi_n(t)) \end{bmatrix}_{nx2}, \tag{A.4}$$

$$\Theta=\begin{bmatrix} c_{t1}\Lambda_1\phi_1\left(\xi_1(t)\right) & c_{t1}\Lambda_1\phi_1\left(\xi_1(t)\right) \\ \vdots & \vdots \\ c_{t1}\Lambda_1\phi_n\left(\xi_1(t)\right) & c_{t2}\Lambda_2\phi_n\left(\xi_2(t)\right) \end{bmatrix}, \tag{A.5}$$

$$\Upsilon=\begin{bmatrix} (-c_{t1}\Lambda_1^2\phi_1^2(\xi_1(t)))-c_{t2}\Lambda_2^2\phi_1^2(\xi_2(t)))/\Omega_1 & \dots & (-c_{t1}\Lambda_1^2\phi_n^2(\xi_1(t)))-c_{t2}\Lambda_2^2\phi_n^2(\xi_2(t)))/\Omega_1 \\ \dots & \dots & \dots \\ (-c_{t1}\Lambda_1^2\phi_1^2(\xi_1(t)))-c_{t2}\Lambda_2^2\phi_1^2(\xi_2(t)))/\Omega_n & \dots & (-c_{t1}\Lambda_1^2\phi_n^2(\xi_1(t)))-c_{t2}\Lambda_2^2\phi_n^2(\xi_2(t)))/\Omega_n \end{bmatrix}, \tag{A.6}$$

$$\Pi=\begin{bmatrix} (-k_{t1}\Lambda_1^2\phi_1^2(\xi_1(t)))-k_{t2}\Lambda_2^2\phi_1^2(\xi_2(t)))/\Omega_1 & \cdots & (-k_{t1}\Lambda_1^2\phi_n^2(\xi_1(t)))-k_{t2}\Lambda_2^2\phi_n^2(\xi_2(t)))/\Omega_1 \\ \vdots & \vdots & \vdots \\ (-k_{t1}\Lambda_1^2\phi_1^2(\xi_1(t)))-k_{t2}\Lambda_2^2\phi_1^2(\xi_2(t)))/\Omega_n & \cdots & (-k_{t1}\Lambda_1^2\phi_n^2(\xi_1(t)))-k_{t2}\Lambda_2^2\phi_n^2(\xi_2(t)))/\Omega_n \end{bmatrix}, \tag{A.7}$$

$$P=\begin{bmatrix} -\Lambda_1\phi_1\left(\xi_1(t)\right)f_{s1}-\Lambda_2\phi_1\left(\xi_2(t)\right)f_{s2} \\ \vdots \\ -\Lambda_1\phi_n\left(\xi_1(t)\right)f_{s1}-\Lambda_2\phi_n\left(\xi_2(t)\right)f_{s2} \end{bmatrix}_{nx1}, \tag{A.8}$$

Table 2. MATLAB the algorithm of r(x) using MATLAB

```
Input      : n_max, n_min, G_d(n_0) , N, n_0 = 0.1, c = 2;
Calculate  : Dn = (n_max - n_min)/ N;   t = t_0 : Dt : t_end;   x = v*t;
             For i = 1, ... , N,
             n_i = n_min + (i-1)*Dn;  % Spatial frequency value
             G_d^i(n) = G_d(n_0) *(n_i / n_0)^-a ;  % PSD function
             r = r + sqrt(4*G_d^i(n)*Dn)*cos(2*pi*n_i*x + rand(1)*2*pi);  % Surface roughness
             end
Output     :r(x)
```